Electronic Supplementary Material (ESI) for RSC Advances.
This journal is © The Royal Society of Chemistry 2021

Supporting information

Architecture of multi-channel and easy-to-make microfluidic paper-based colorimetric device (μPCD) towards selective and sensitive recognition of uric acid by AuNPs: An innovative portable tool for the rapid and low-cost identification of clinically relevant biomolecules

Fatemeh Farshchi [a,b], Arezoo Saadati [c], Mohammad Hasanzadeh [b,*], Farzad Seidi [a**]

[a] Jiangsu Co-Innovation Center for Efficient Processing and Utilization of Forest Resources and International Innovation Center for Forest Chemicals and Materials, Nanjing Forestry University, Nanjing 210037, China.

[b] Pharmaceutical Analysis Research Center, Tabriz University of Medical Sciences, Tabriz, Iran.

[c] Drug Applied Research Center, Tabriz University of Medical Sciences, Tabriz, Iran.

Corresponding Author

* (Mohammad Hasanzadeh) Pharmaceutical Analysis Research Center, Tabriz University of Medical Sciences, Tabriz, Iran.
E-mail address: (*) hasanzadehm@tbzmed.ac.ir

** (Farzad Seidi) Jiangsu Co-Innovation Center for Efficient Processing and Utilization of Forest Resources and International Innovation Center for Forest Chemicals and Materials, Nanjing Forestry University, Nanjing 210037, China E-mail address: (**) f_seidi@njfu.edu.cn

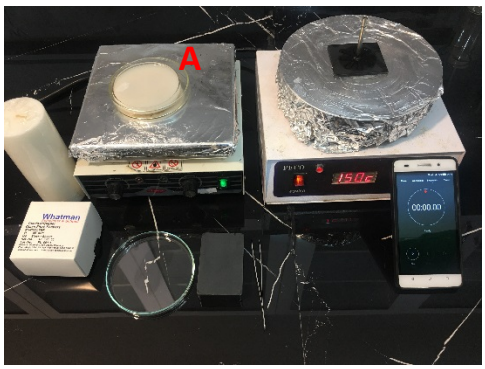
A
PECO
150c
00:00.00
Whatman

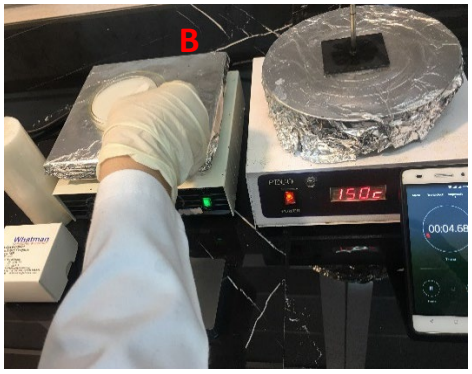
B
PECO
150c
00:04.68
Whatman

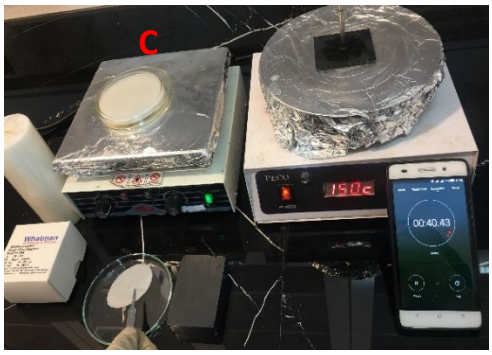
C
PECO
150c
00:40.43
Whatman

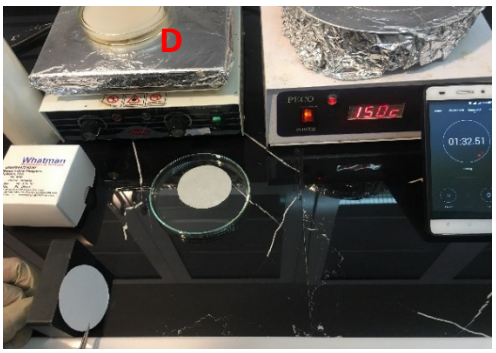
D
PECO
150c
01:32.51
Whatman

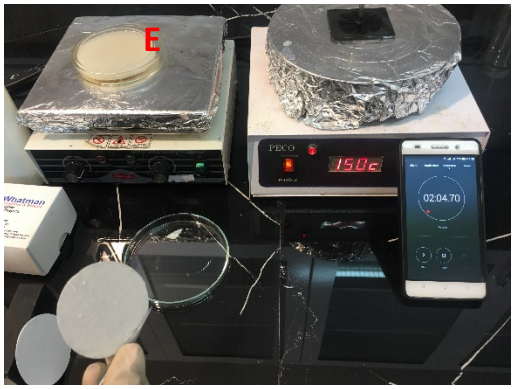
E
PECO
150c
02:04.70
Whatman

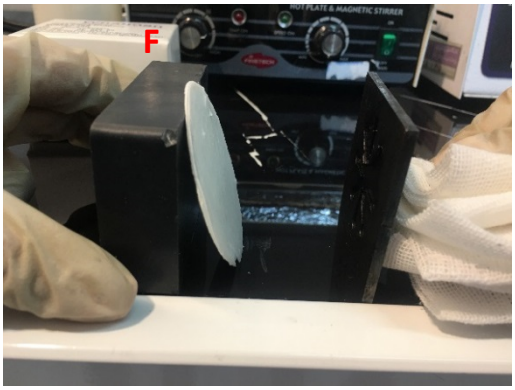
F
HOTPLATE & MAGNETIC STIRRER

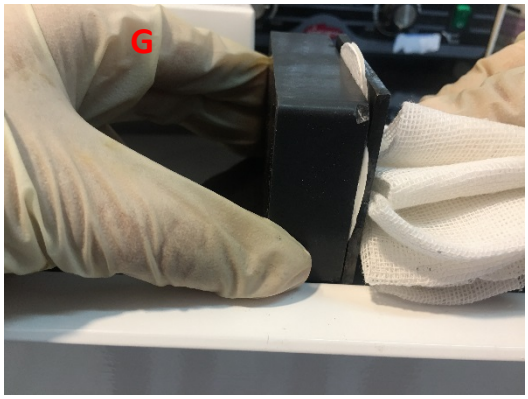
G

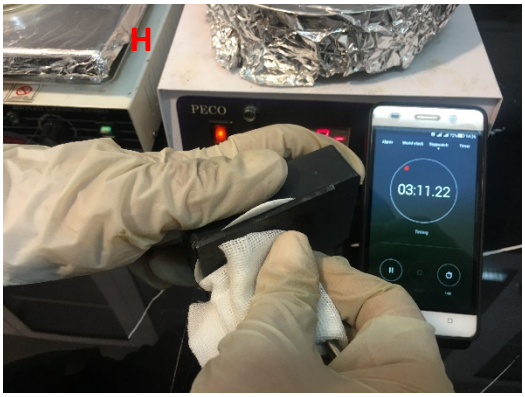
H
PECO
03:11.22

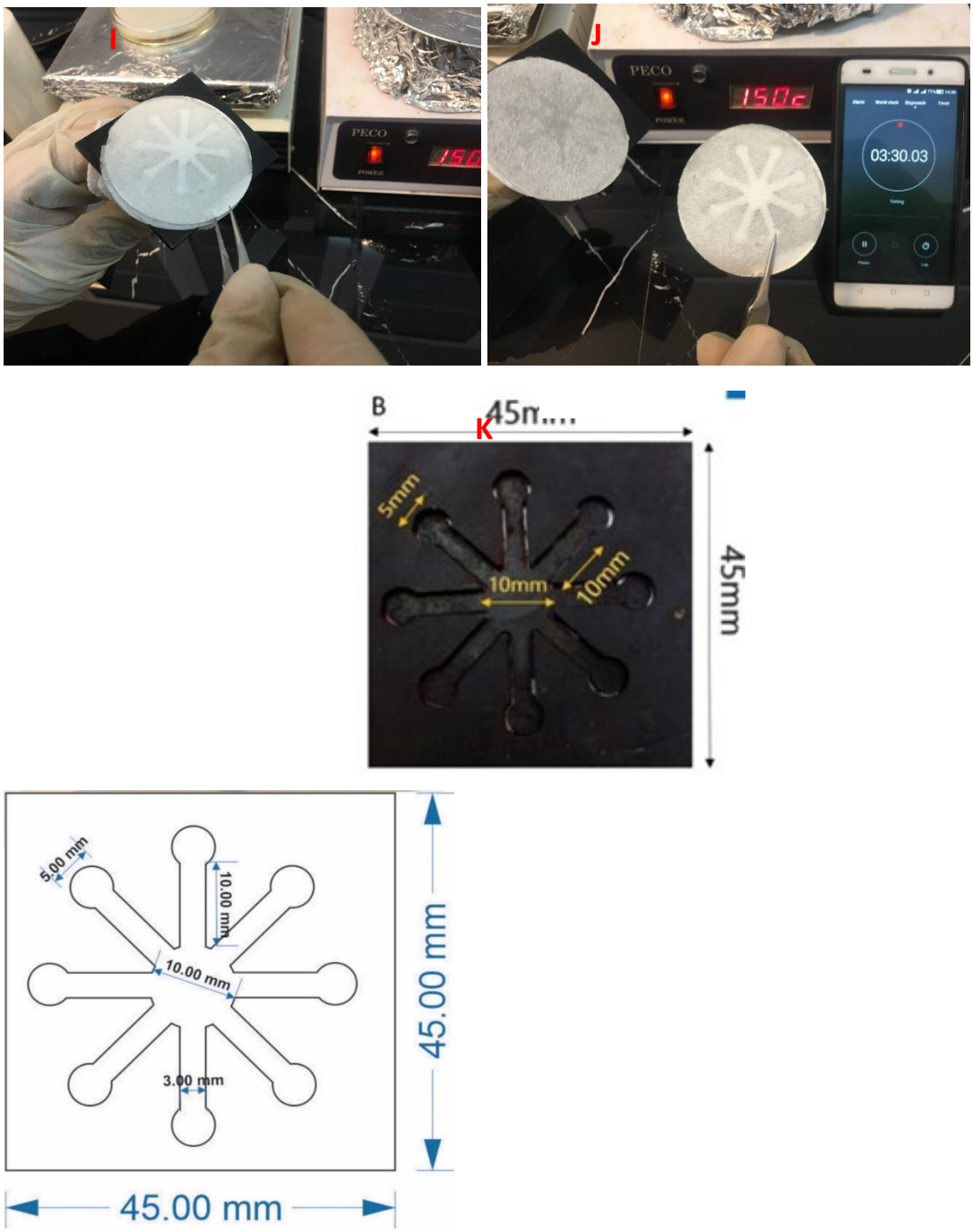

Fig. S1. *The fabrication process of paper-based microfluidic device, A) Materials and equipment required B) Immersion of fiberglass paper in molten paraffin at 90 ° C, C) Dry paraffin-impregnated paper at room temperature, D) Place paraffin-free paper between paraffin-containing paper and a magnet, E) Place paraffin paper on the paraffin-free paper F)Place paraffin-free paper and paraffin-containing paper between the iron pattern and the magnet, G) Attract the pattern to the magnet H) Separation of pattern and magnet I) Formation of microfluidic channels in paraffin-free paper, J) Made paper-based microfluidic device K) Designed pattern size.*

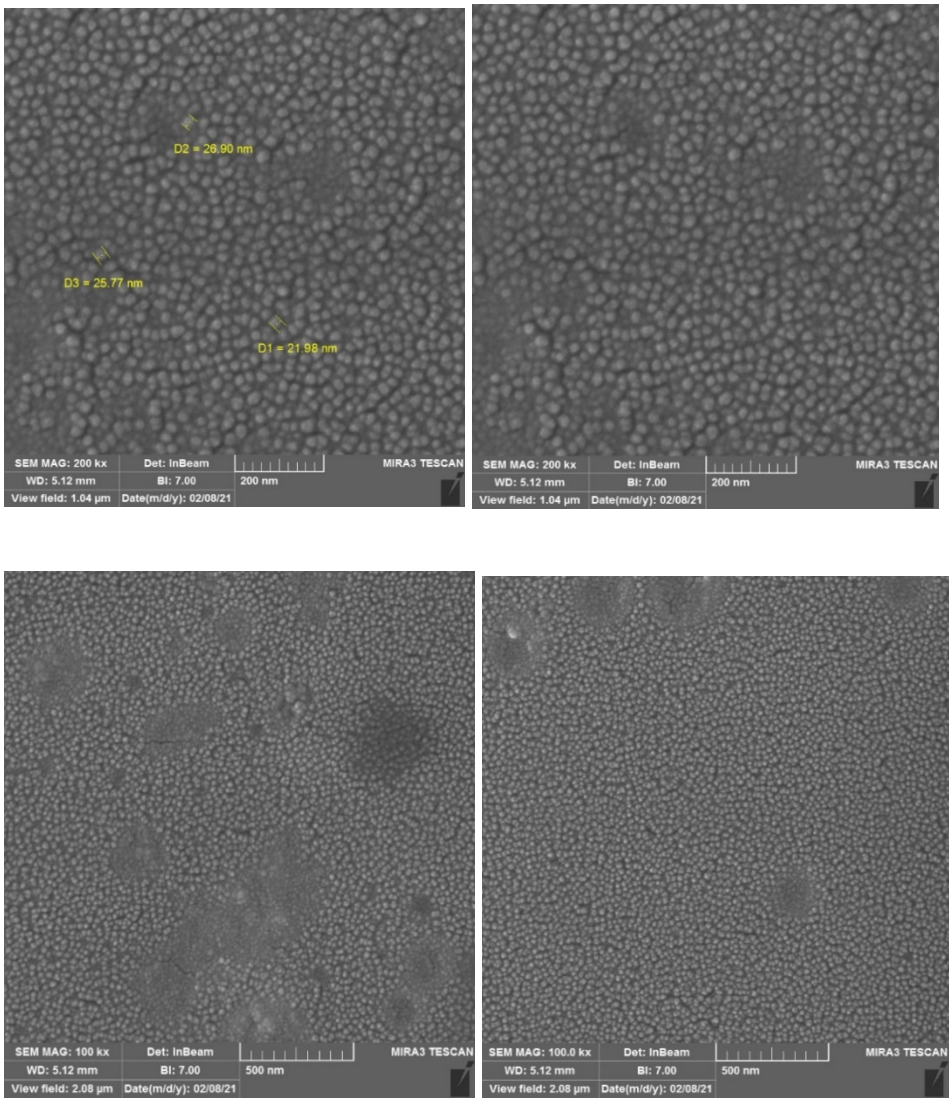

Fig. S2. *FE-SEM images of AuNPs-CysA.*

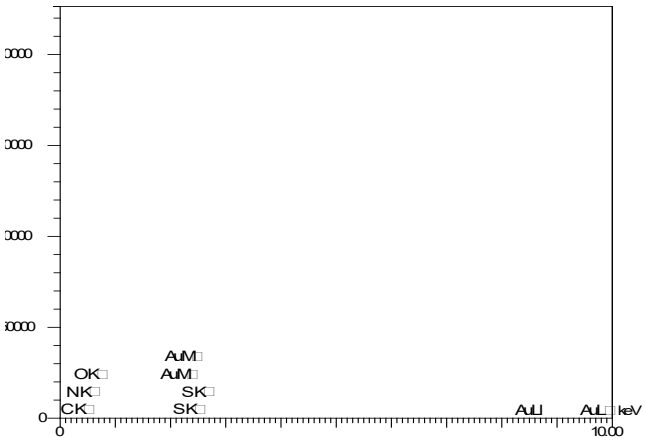

Fig. S3. *EDC images of AuNPs-CysA.*

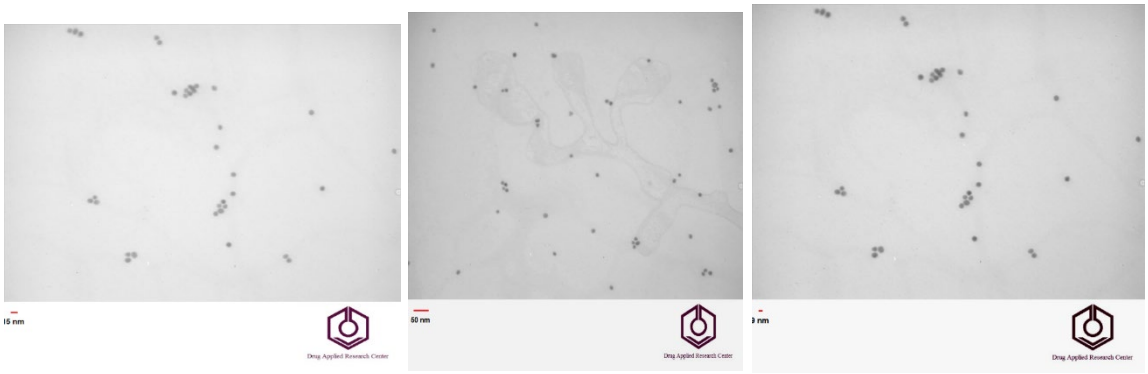

Fig. S4. *TEM images of AuNPs-CysA.*

A

		Size (d.n...	% Number:	St Dev (d.n...
Z-Average (d.nm): 97.87	**Peak 1:**	15.38	100.0	3.722
PdI: 0.641	**Peak 2:**	0.000	0.0	0.000
Intercept: 0.615	**Peak 3:**	0.000	0.0	0.000

Result quality Refer to quality report

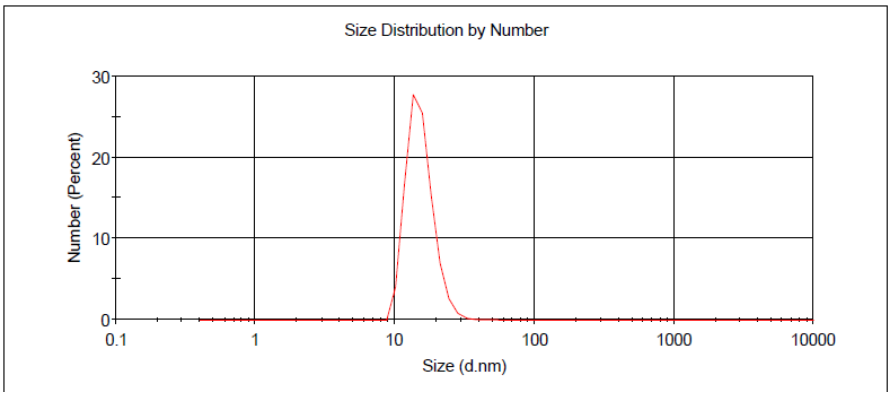

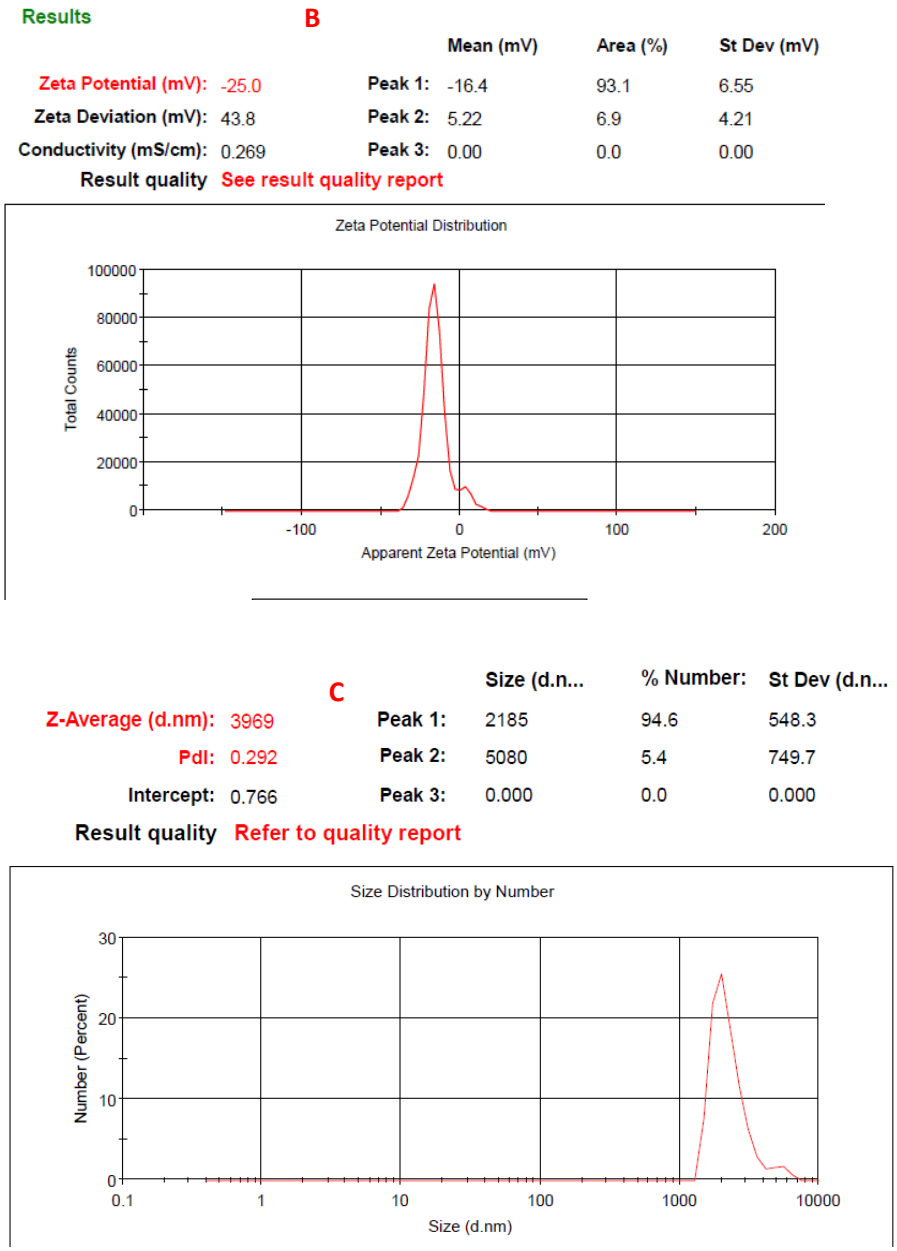

Fig. S5 *A) Size distribution analysis of AuNPs-CysA by DLS. B) Recorded Zp for synthesized AuNPs-CysA, C) Size distribution analysis of AuNPs-CysA combined with UA.*

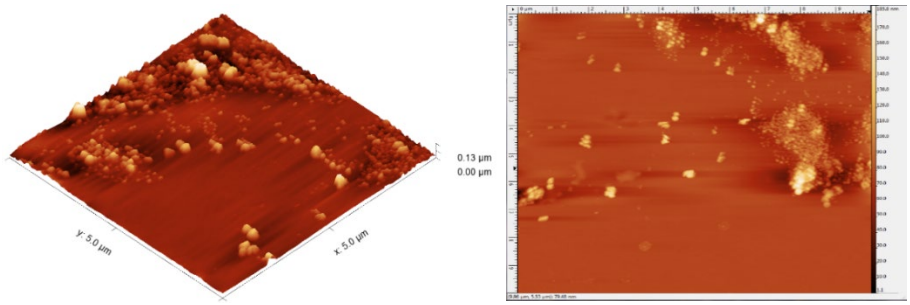

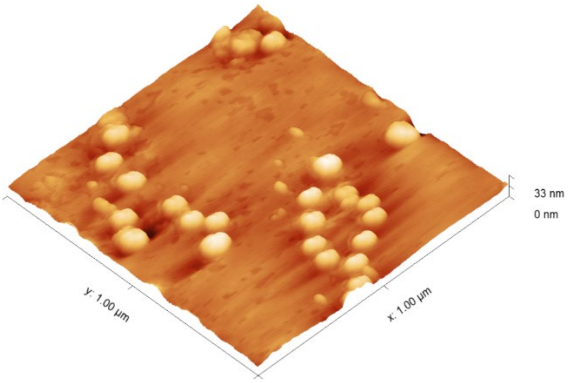

Fig. S6. *AFM images of AuNPs-CysA.*

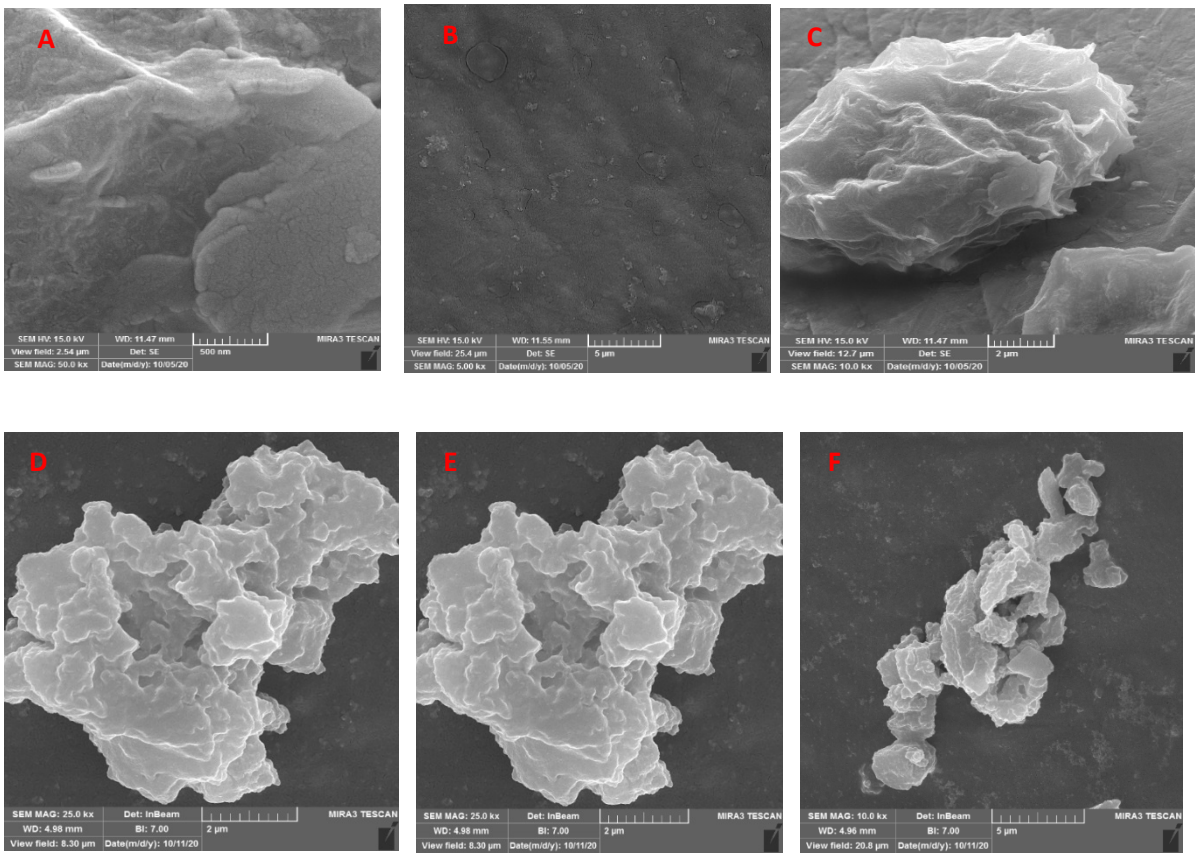

Fig. S7. A-C) *FE-SEM images of AuNFs synthesized in pH = 6.15, D-F) pH = 4.19 in different magnification, respectively.*

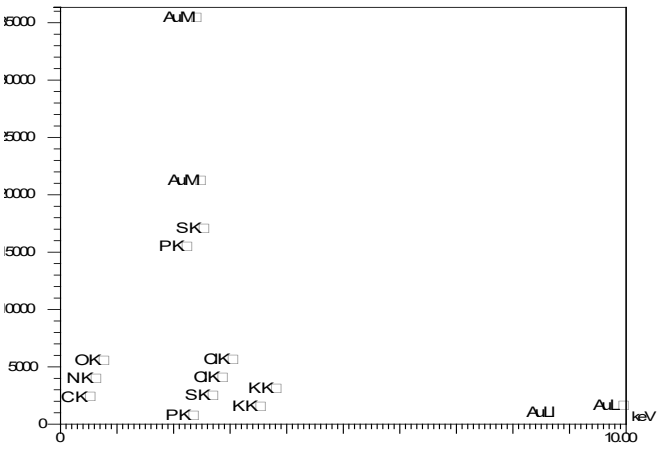

Fig. S8. *EDC images of AuNFs.*

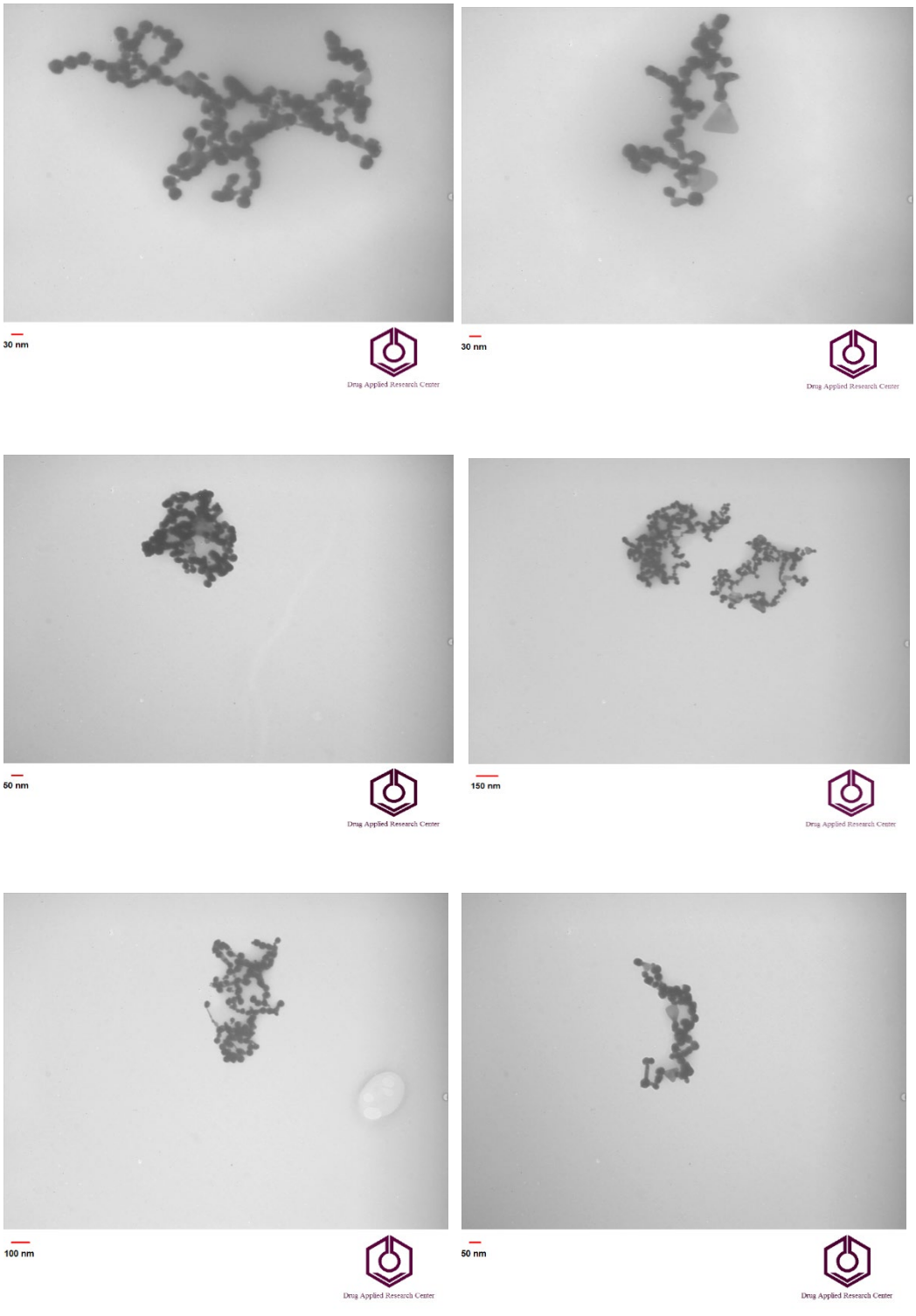

Fig. S9. *TEM images of AuNFs.*

Results

A

			Size (d.n...	% Number:	St Dev (d.n...
Z-Average (d.nm):	303.2	Peak 1:	150.1	100.0	113.9
PdI:	0.340	Peak 2:	0.000	0.0	0.000
Intercept:	0.768	Peak 3:	0.000	0.0	0.000

Result quality Refer to quality report

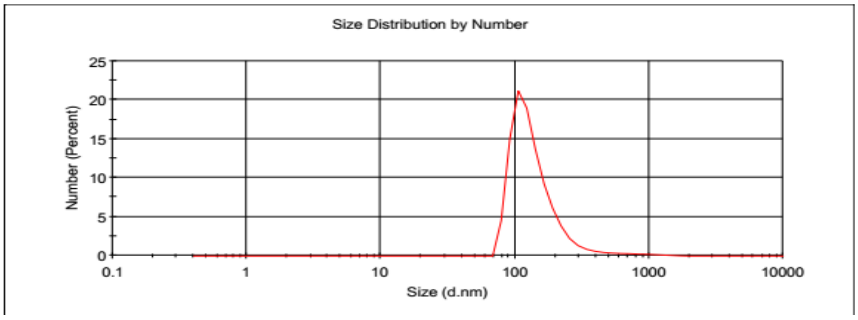

Results

B

			Size (d.n...	% Number:	St Dev (d.n...
Z-Average (d.nm):	94.31	Peak 1:	71.86	0.0	24.77
PdI:	0.316	Peak 2:	11.33	100.0	2.574
Intercept:	0.820	Peak 3:	0.000	0.0	0.000

Result quality Refer to quality report

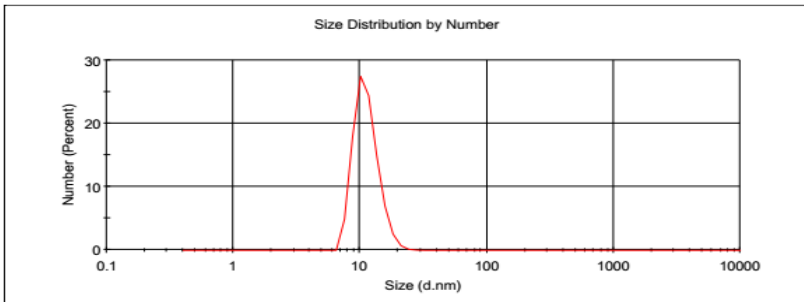

C

			Size (d.nm):	% Volume:	St Dev (d.nm):
Z-Average (d.nm):	2816	Peak 1:	3232	100.0	998.3
PdI:	0.015	Peak 2:	0.000	0.0	0.000
Intercept:	0.724	Peak 3:	0.000	0.0	0.000

Result quality Refer to quality report

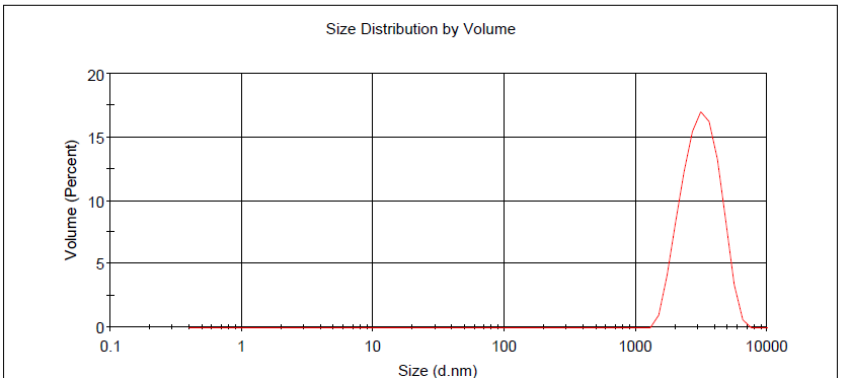

D

		Size (d.n...	% Intensity:	St Dev (d.n...
Z-Average (d.nm): 1736	Peak 1:	1578	100.0	365.8
PdI: 0.322	Peak 2:	0.000	0.0	0.000
Intercept: 0.766	Peak 3:	0.000	0.0	0.000

Result quality Refer to quality report

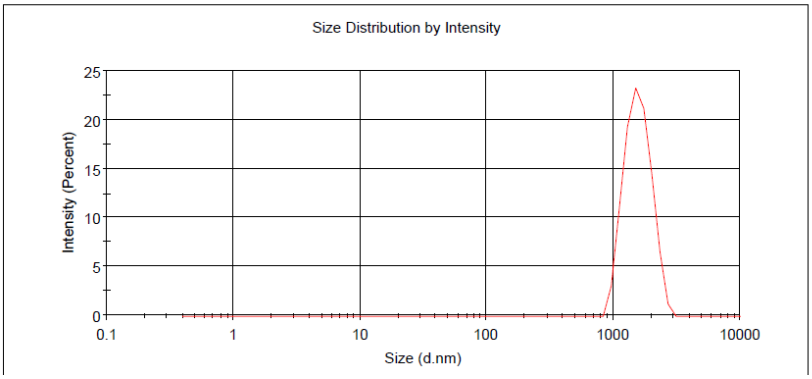

Results

E

		Mean (mV)	Area (%)	St Dev (mV)
Zeta Potential (mV): 23.9	Peak 1:	23.9	100.0	4.80
Zeta Deviation (mV): 4.80	Peak 2:	0.00	0.0	0.00
Conductivity (mS/cm): 0.368	Peak 3:	0.00	0.0	0.00

Result quality Good

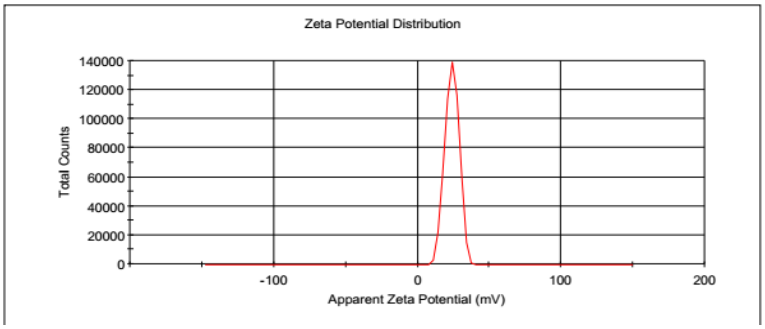

Results

F

		Mean (mV)	Area (%)	St Dev (mV)
Zeta Potential (mV): -9.31	Peak 1:	-9.31	100.0	4.65
Zeta Deviation (mV): 4.65	Peak 2:	0.00	0.0	0.00
Conductivity (mS/cm): 0.492	Peak 3:	0.00	0.0	0.00

Result quality Good

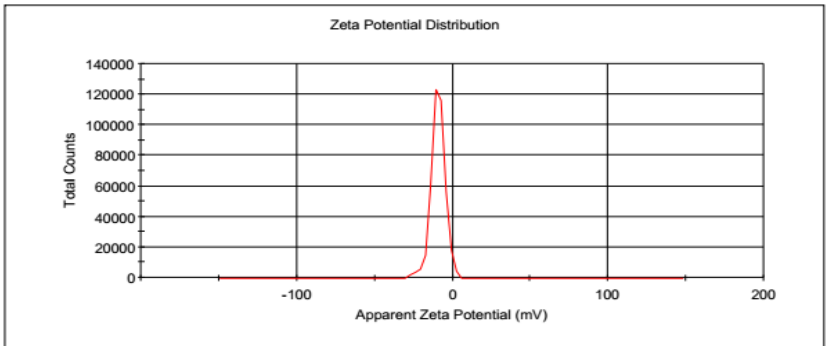

Fig. S10. A-B) *Size distribution analysis of AuNFs* ***C-D)*** *Size distribution analysis of AuNFs after the combination with UA by DLS* ***E-F)*** *Recorded Zp for synthesized AuNFs in the pH = 4.91 and pH = 6.15, respectively.*

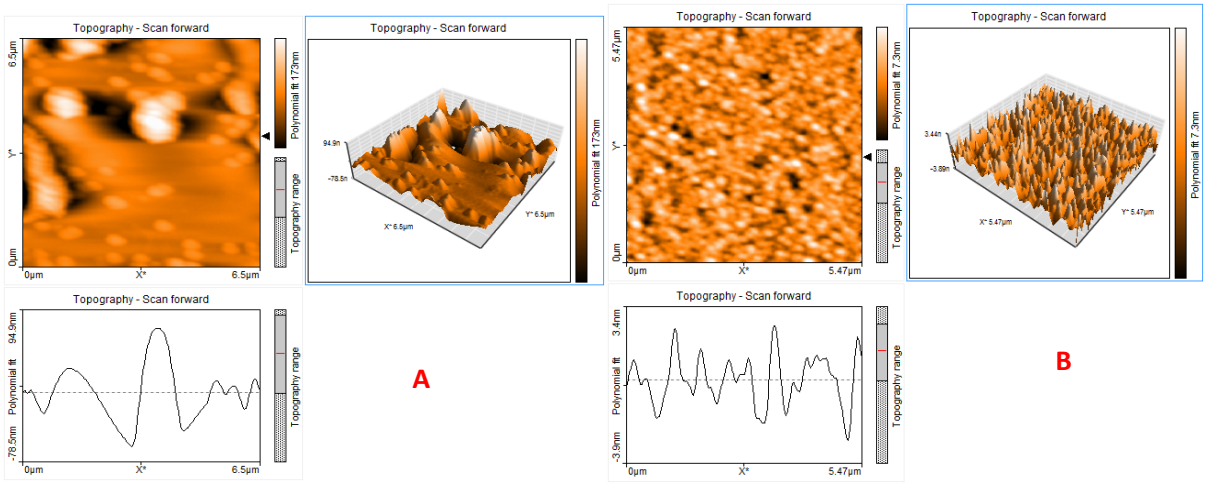

Fig. S11. A-B) *AFM images of synthesized AuNFs prepared in the pH of 4.91 and 6.15, respectively.*

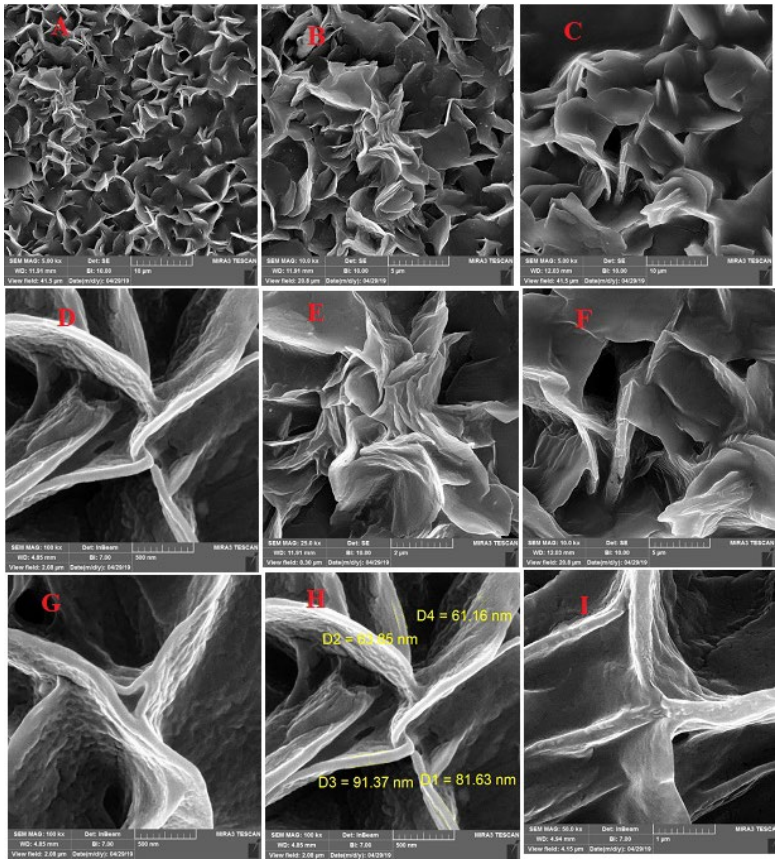

Fig. S12. *FE-SEM images of GNSs in different magnification.*

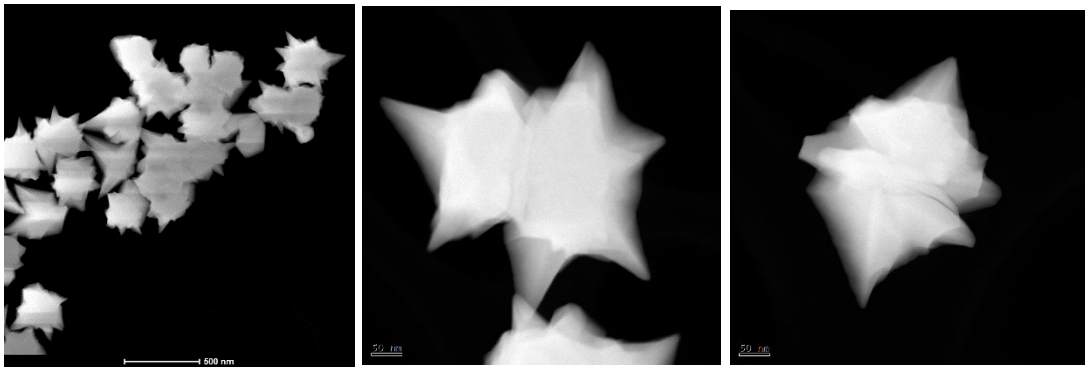

Fig. S13. *TEM images of GNSs in various magnification.*

A

Results

			Size (d.n...	% Number:	St Dev (d.n...
Z-Average (d.nm):	135.5	Peak 1:	24.61	100.0	6.831
PdI:	0.393	Peak 2:	0.000	0.0	0.000
Intercept:	0.649	Peak 3:	0.000	0.0	0.000

Result quality Good

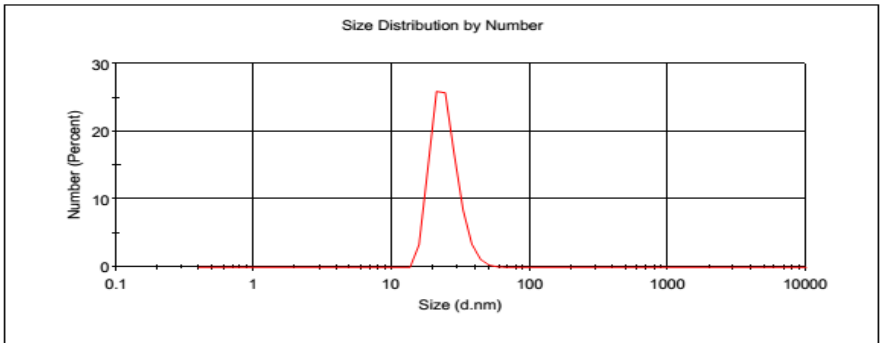

B

			Size (d.n...	% Number:	St Dev (d.n...
Z-Average (d.nm):	930.3	Peak 1:	430.1	0.2	73.05
PdI:	0.616	Peak 2:	59.31	99.8	9.318
Intercept:	0.841	Peak 3:	0.000	0.0	0.000

Result quality Refer to quality report

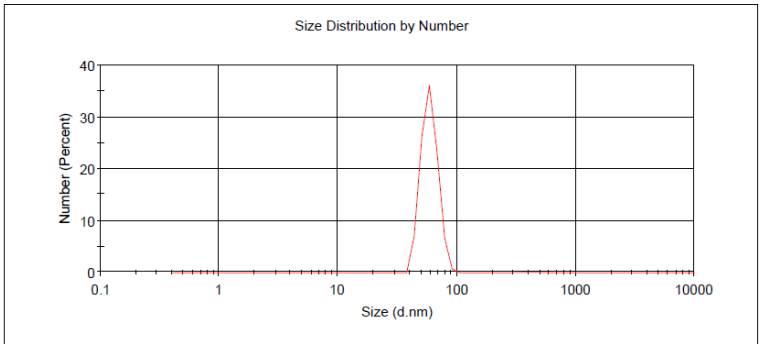

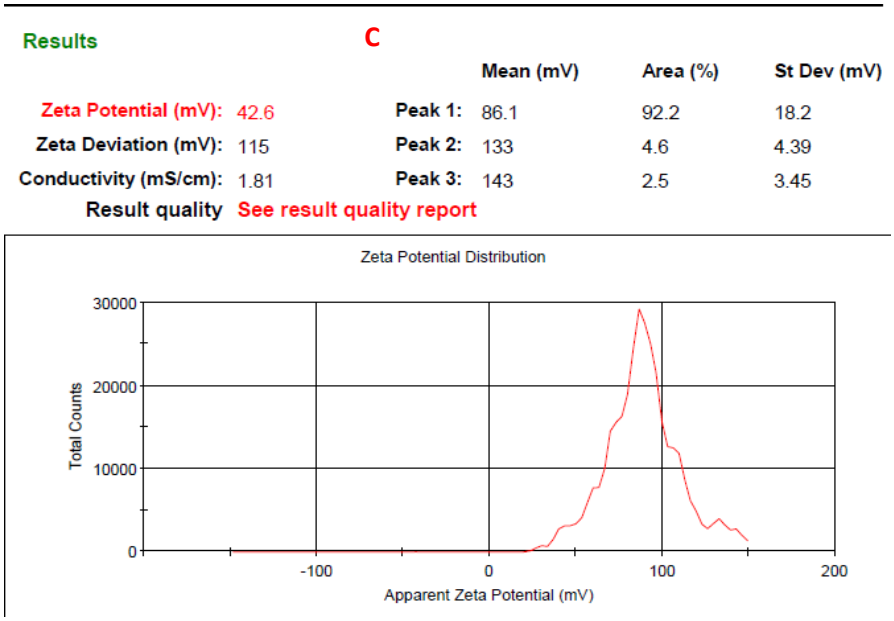

Fig. S14. A) *Size distribution analysis of GNSs* ***B)*** *Size distribution analysis of GNSs with UA by DLS* ***C)*** *Recorded Zp for synthesized GNSs.*

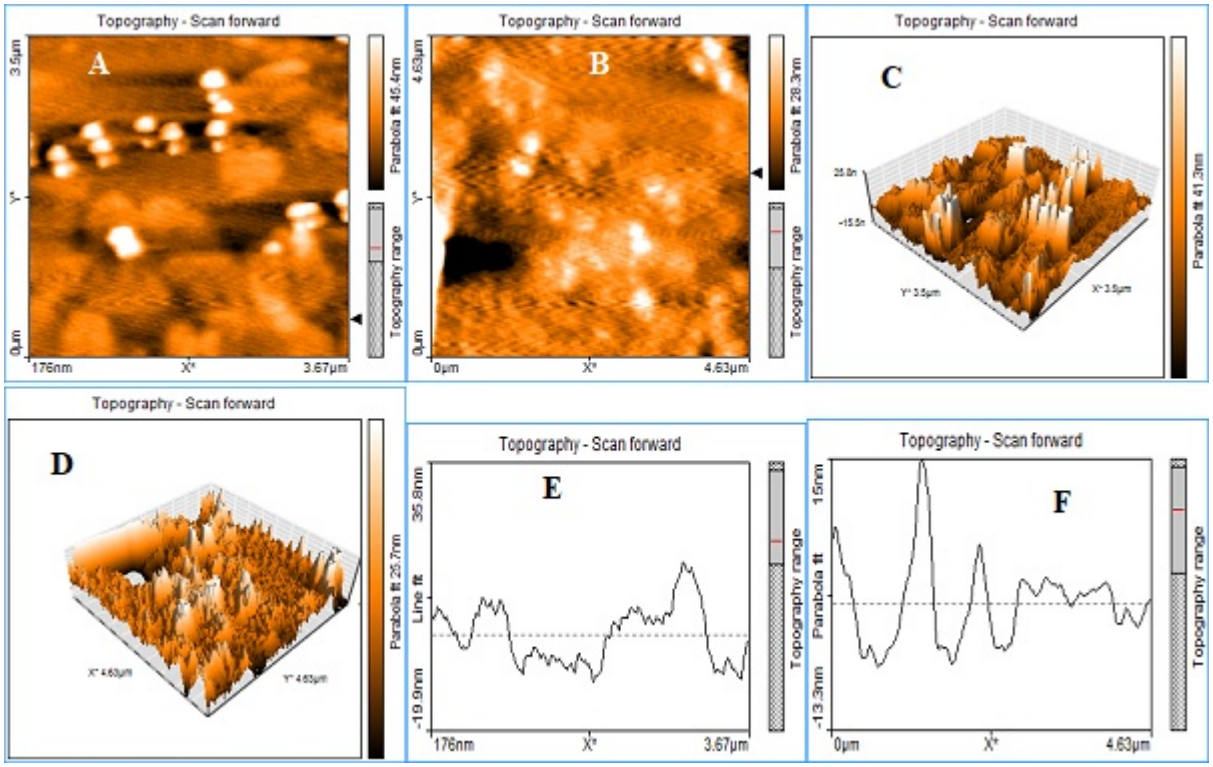

Fig. S15. *AFM imaging of synthesized GNSs after covering on the slide.*

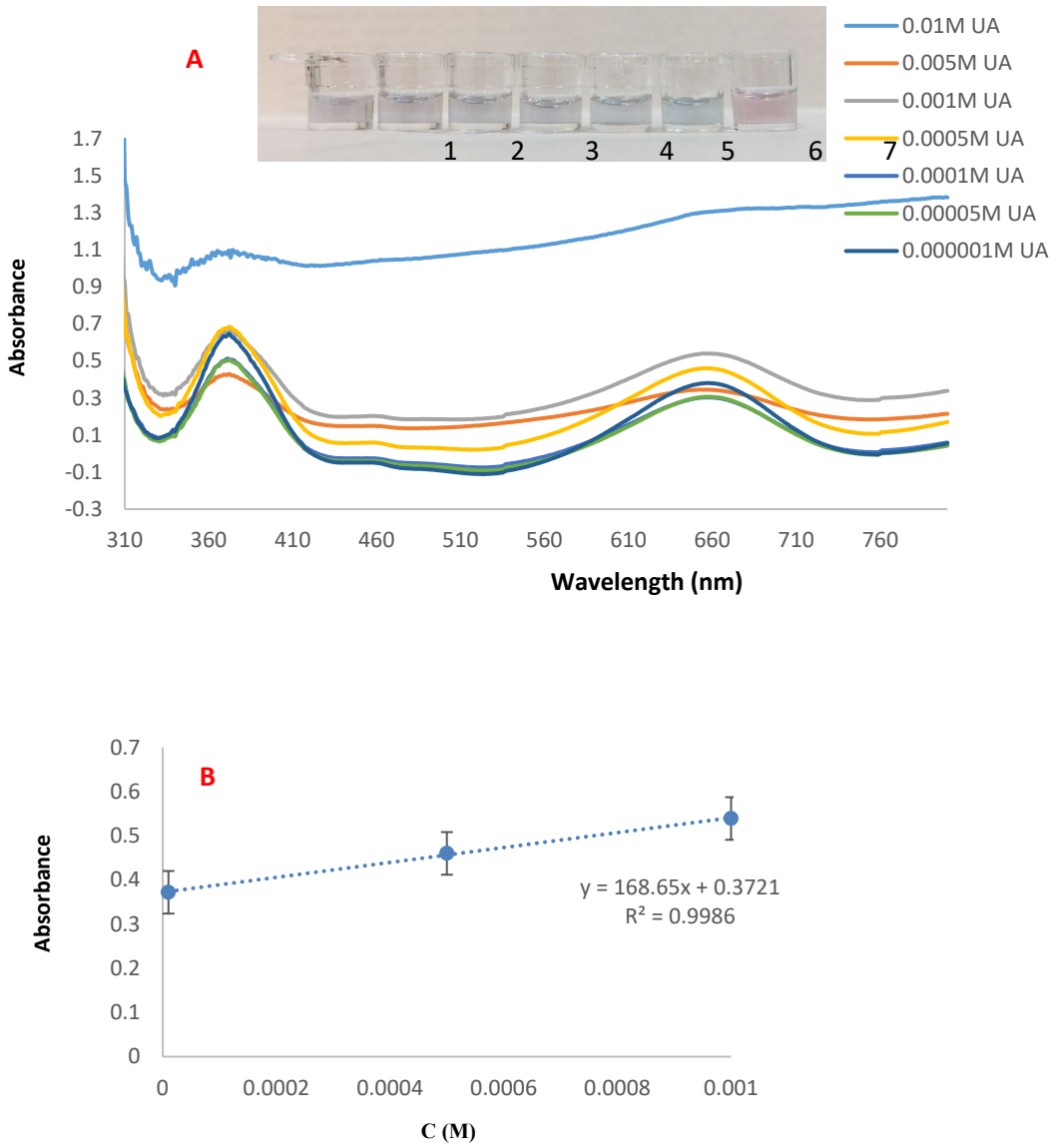

Fig. S16. A) *Photographic image and UV-Vis spectra recorded from reaction systems containing AuNPs-CysA, (TMB+H_2O_2+Met) and different concentration of UA (0.01, 0.005, 0.001, 0.0005, 0.0001, 0.00005 and 0.000001 M),* ***B)*** *Calibration curve of peak intensity versus concentration of UA.*

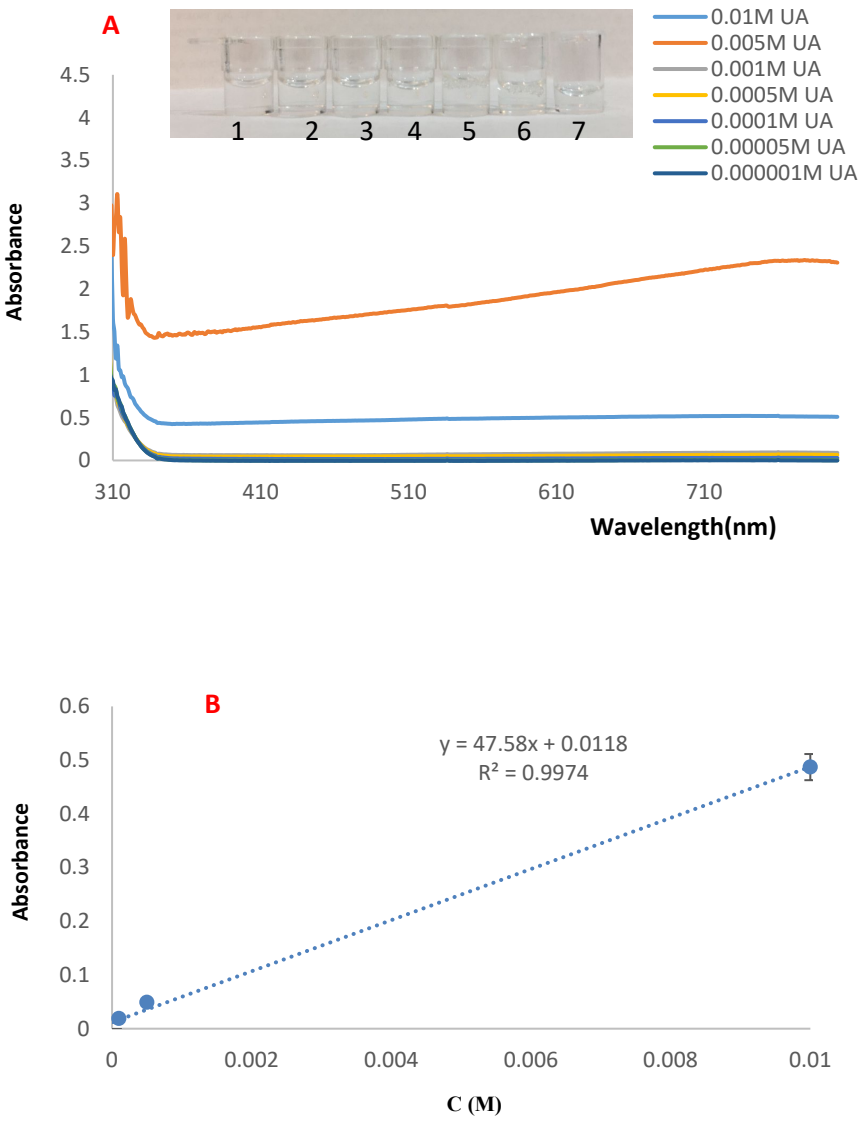

Fig. S17. A) *Photographic image and UV-Vis spectra recorded from reaction systems containing GNSs, (TMB+H_2O_2+Met) and different concentration of UA (0.01, 0.005, 0.001, 0.0005, 0.0001, 0.00005 and 0.000001 M),* ***B)*** *Calibration curve of peak intensity versus concentration of UA.*

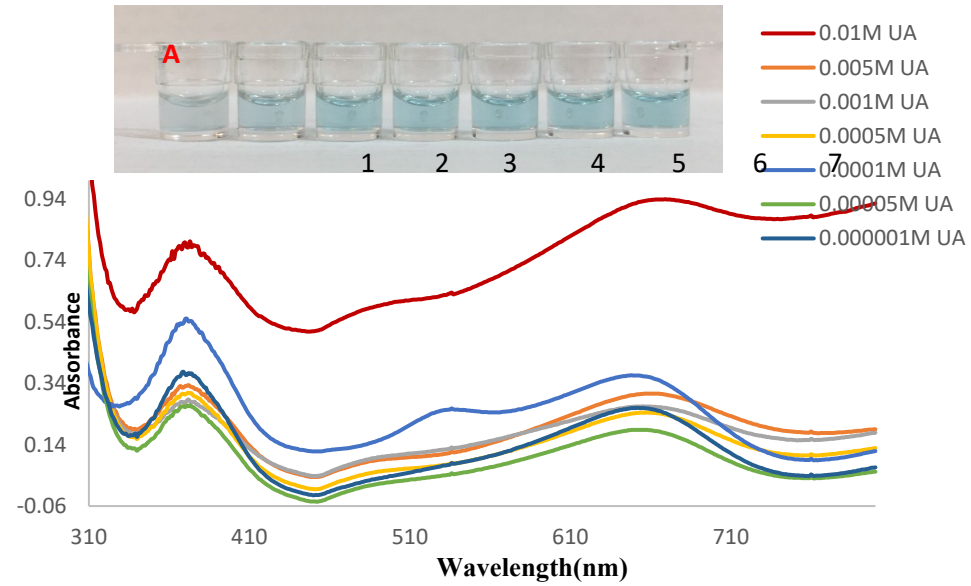

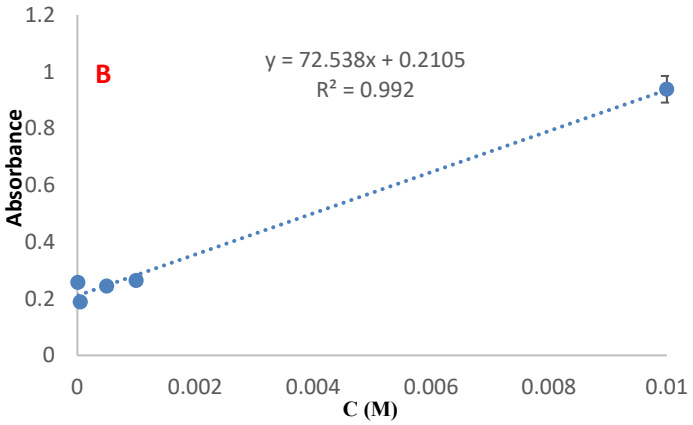

Fig. S18. A) *Photographic image and UV-Vis spectra recorded from reaction systems containing AuNFs (Ph = 4.91) (TMB+H_2O_2+Met) and different concentration of UA (0.01, 0.005, 0.001, 0.0005, 0.0001, 0.00005 and 0.000001 M),* ***B)*** *Calibration curve of peak intensity versus concentration of UA.*

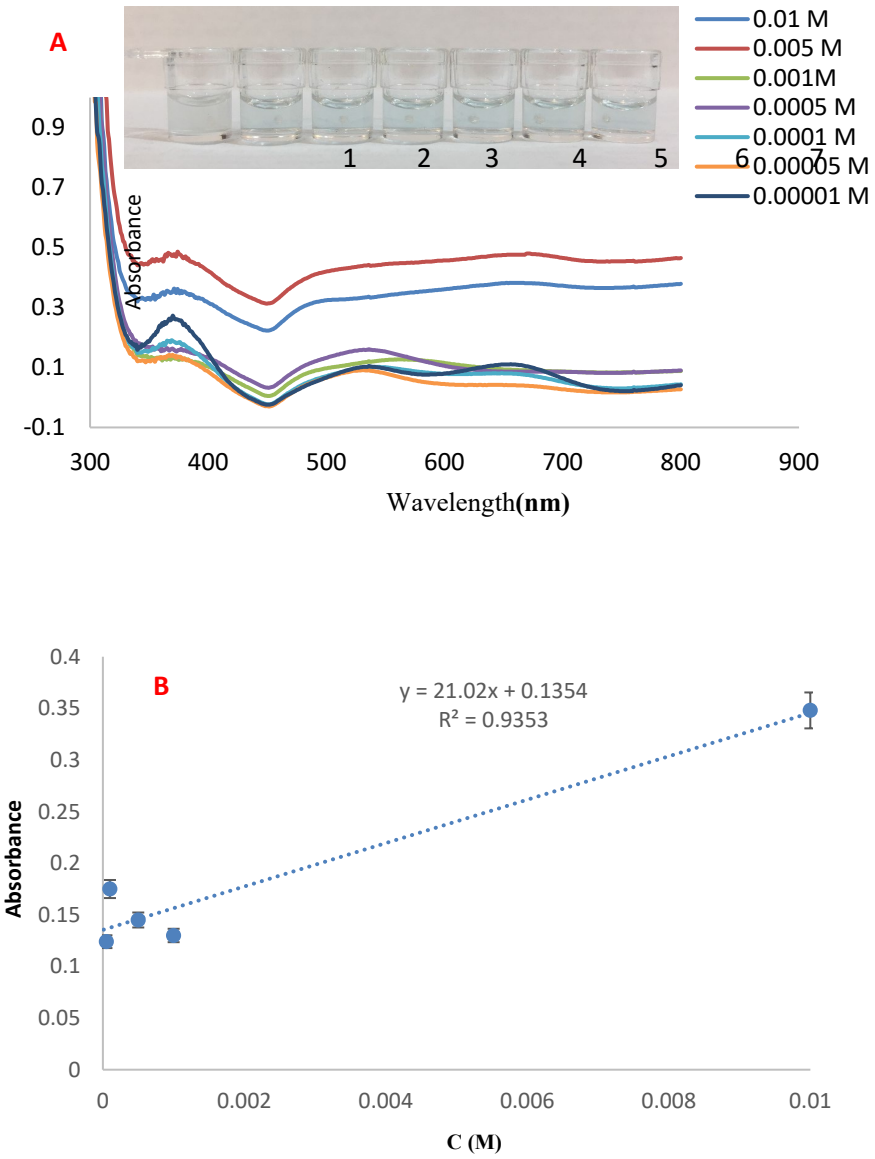

Fig. S19. A) *Photographic image and UV-Vis spectra recorded from reaction systems containing AuNFs (pH = 6.15) (TMB+H_2O_2+Met) and different concentration of UA (0.01, 0.005, 0.001, 0.0005, 0.0001, 0.00005 and 0.000001 M),* ***B)*** *Calibration curve of peak intensity versus concentration of UA.*

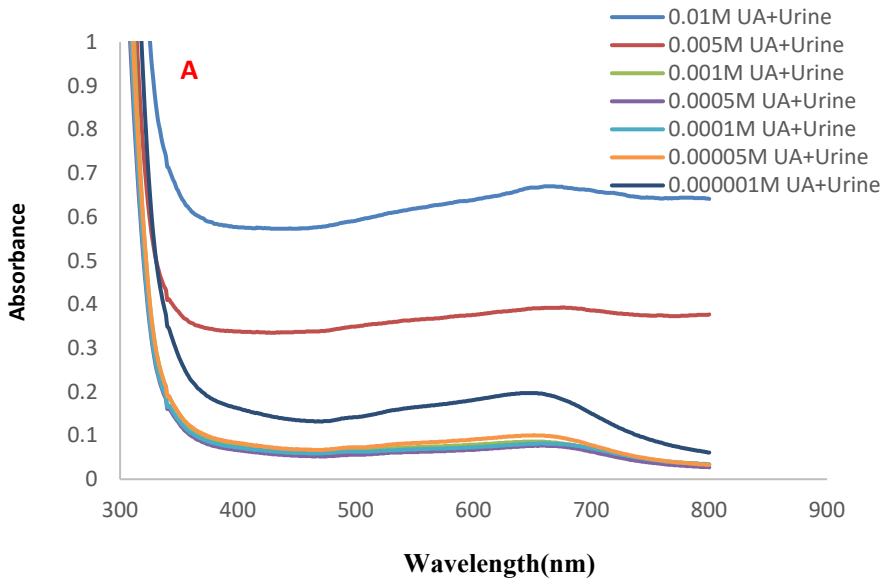

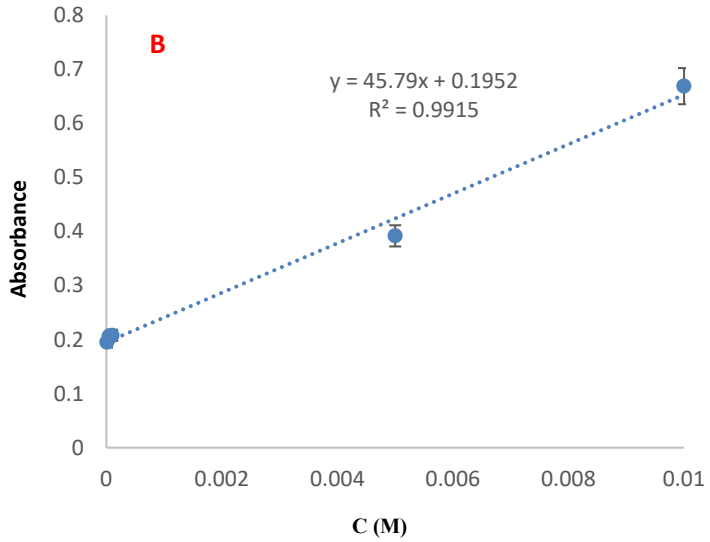

Fig. S20. A) *Absorption response for UA with increasing concentrations (0.00005 to 0.01 M) and AuNPs-CysA in human urine specimens,* ***B)*** *Calibration plot of peak intensity versus concentration of UA.*

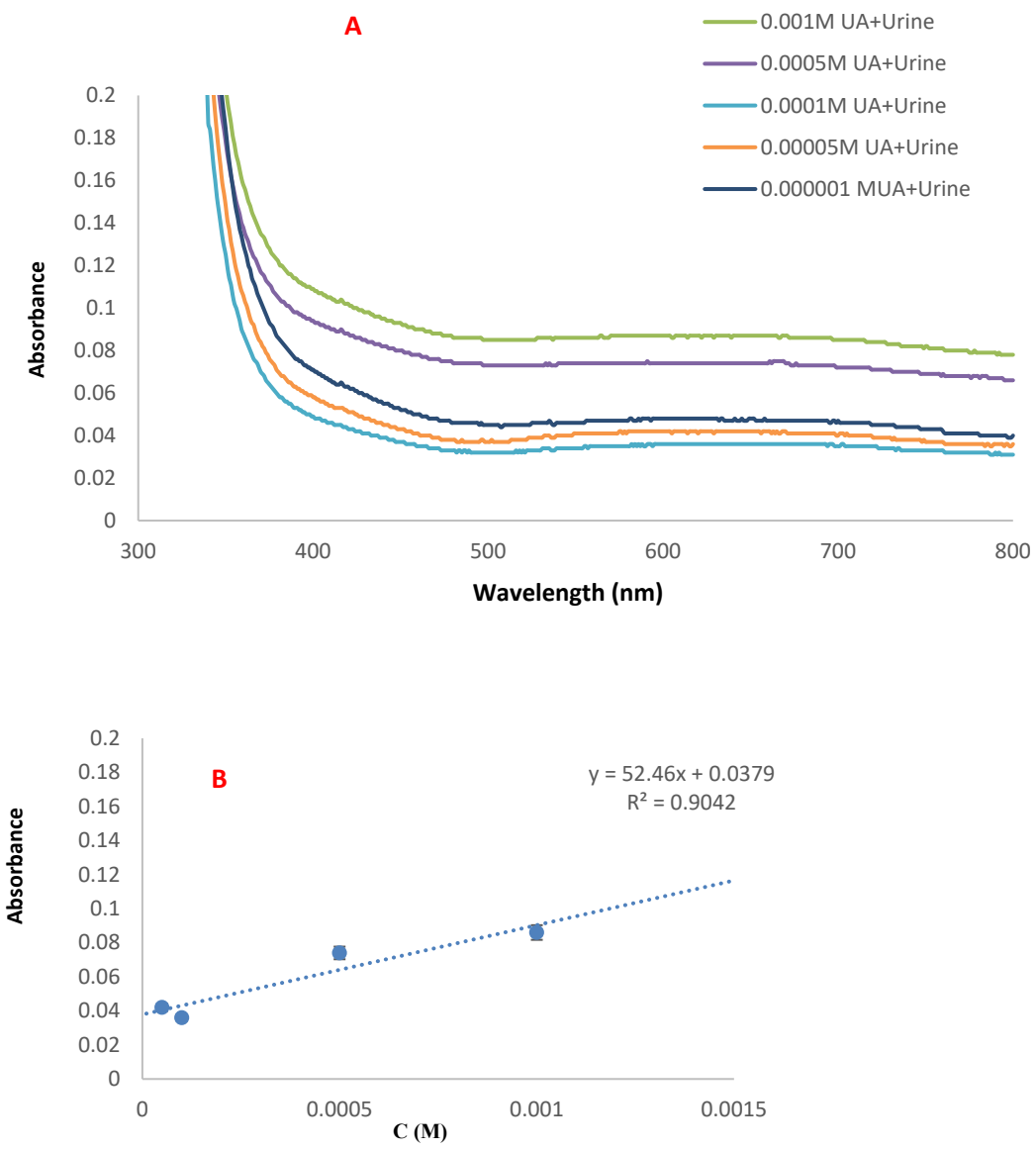

Fig. S21. A) *Absorption response for UA with increasing concentrations (0.000001 to 0.001 M) and GNSs in human urine specimens,* ***B)*** *Calibration plot of peak intensity versus concentration of UA.*

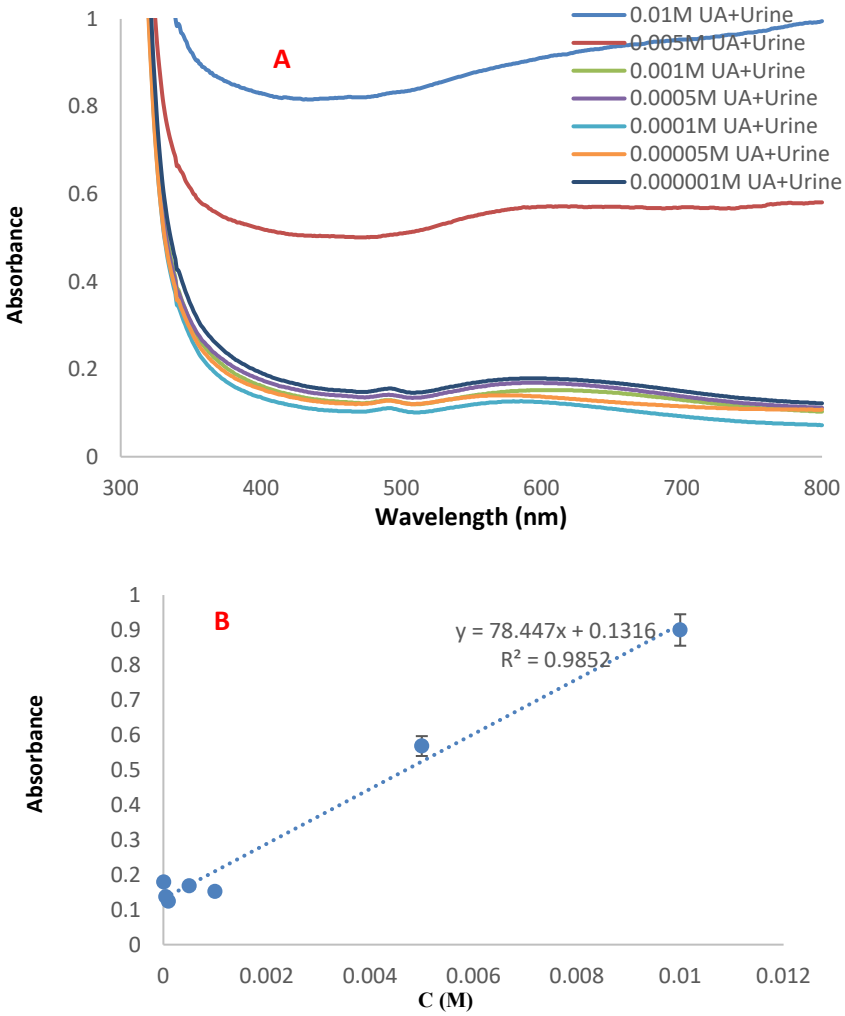

Fig. S22. A) *Absorption response for UA with increasing concentrations (0.000001 to 0.01 M) and AuNFs pH=4.91 in human urine specimens,* ***B)*** *Calibration plot of peak intensity versus concentration of UA.*

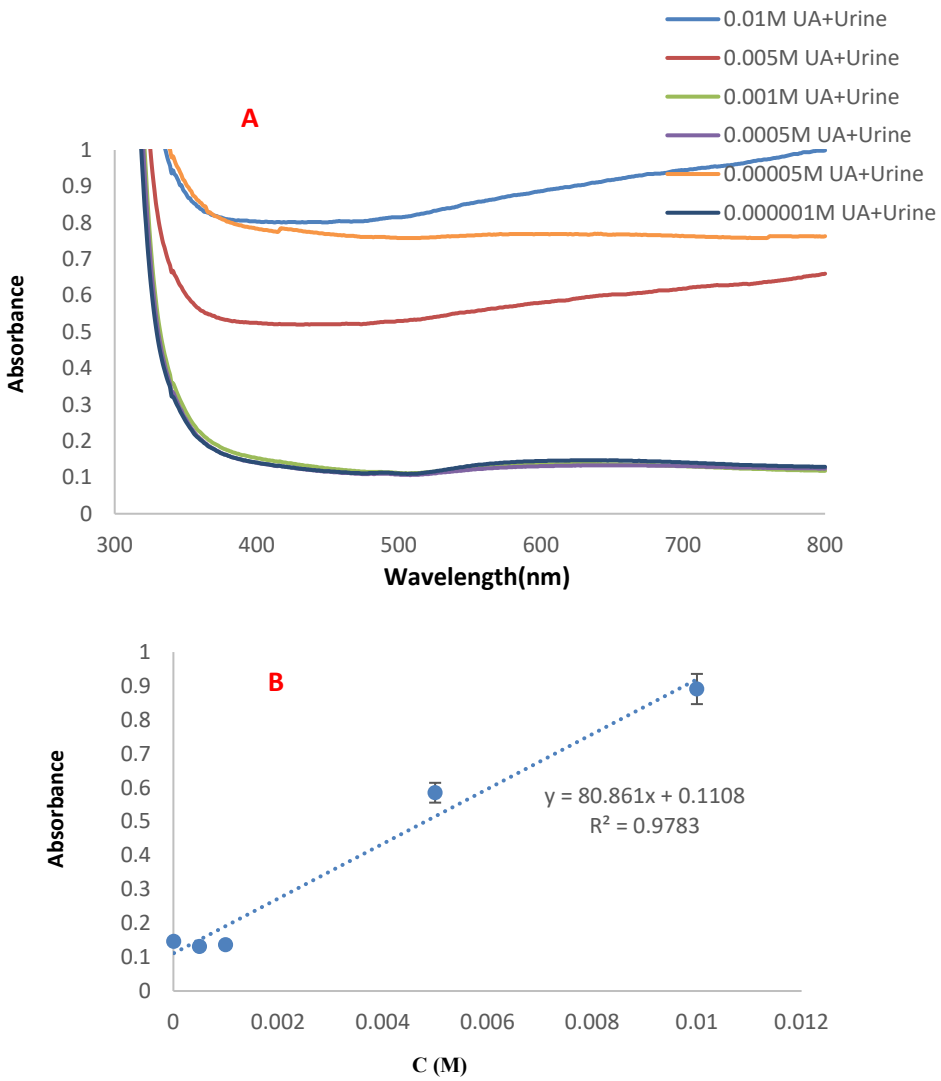

Fig. S23. A) *Absorption response for UA with increasing concentrations (0.000001 to 0.01 M) and AuNFs pH=6.15 in human urine specimens,* ***B)*** *Calibration plot of peak intensity versus concentration of UA.*

Table S1. *Analytical Figure of merits.*

Type of AuNPs	Linear range (M)	LLOQ(M)
AuNPs-CysA	10^{-6} to 10^{-3}	10^{-6}
GNSs	10^{-4} to 10^{-2}	10^{-4}
AuNFs prepared in pH=4.91	10^{-6} to 10^{-2}	10^{-6}
AuNFs prepared in pH=6.15	5×10^{-5} to 10^{-2}	5×10^{-5}